

Effect of Number of Paris Law Parameters on Bayesian Inference for Remaining Useful Life Estimation

Alexandra Coppe¹, Raphael T. Haftka², and Nam-Ho Kim³
University of Florida, Gainesville, FL, 32611

Information on damage sizes obtained from structural health monitoring (SHM) can be used to estimate remaining useful life (RUL). Damage growth information may also be used to reduce uncertainty in the material properties that govern damage propagation for the structure being monitored, turning aircraft into flying fatigue laboratories. These properties are often widely distributed between nominally identical structures because of manufacturing variability and aging effects. The reduced uncertainty in damage growth characteristics reduces in turn uncertainty in prediction of the RUL of the monitored structural component. It can also help in anticipating damage growth on similar components. Bayesian inference has been used for progressively reducing the uncertainty in structure-specific damage growth parameters in spite of noise and bias in sensor measurements. However, the approach to Bayesian updating we are using here can be computationally intensive, in particular when it comes to updating multiple variables. In this paper we compare updating the two parameters that characterize crack growth in Paris law to updating only one and taking advantage of the correlation between the two. We find that there is little to be gained by updating both parameters.

Nomenclature

ΔK	=	Range of stress intensity factor
$\Delta\sigma$	=	Range of applied stress
Δp	=	Pressure differential
a	=	Half damage size
a_C	=	Critical crack size
a_i	=	Initial crack size
a_N	=	Crack size at N^{th} inspection
a_N^{meas}	=	Measure crack size at N^{th} inspection
a_N^{true}	=	Modeled crack size at N^{th} inspection
b	=	Bias in measurements
C	=	Paris law parameter
K_{IC}	=	Fracture toughness
m	=	Paris law exponent
N	=	Number of cycles
N_f	=	Remaining useful number of cycles
r	=	Fuselage radius
t	=	Panel thickness
v	=	Noise in measurements

¹ Assistant Research Scientist, CALCE Mechanical engineering department, University of Maryland, College Park, MD, 32611, AIAA Student Member.

² Distinguished Professor, Mechanical and Aerospace Engineering department, University of Florida, Gainesville, FL, 32611, AIAA Fellow.

³ Associate Professor, Mechanical and Aerospace Engineering department, University of Florida, Gainesville, FL, 32611, AIAA Member.

V = Amplitude of noise in measurements

I. Introduction

STRUCTURAL health monitoring (SHM) will have significant impact on increasing safety as well as reducing operating and maintenance costs by providing an accurate quantification of degradation and damage at an early stage to reduce or eliminate malfunctions. Furthermore, SHM will allow predictions of the structure's health status and remaining useful life (RUL) without intrusive and time consuming inspections. Continual on-line SHM is based on dynamic processes through the diagnosis of early damage detection, then prognosis of health status and remaining life.

Once damage reaches detectable size, various SHM techniques can be employed to evaluate the current state of structural health by measuring its size¹. In physics-based prognosis techniques, it is necessary to incorporate the measured data into a damage growth model to predict the future behavior of the damage.

The current technology of diagnosis and prognosis using SHM anticipates difficulties associated with uncertainties in sensor data, damage growth models, and material and geometric properties. The first is related to identifying the current health status, while the others are related to predicting the health status in the future. Uncertainties in sensor data can be classified in two categories: systematic departure due to bias and random variability due to noise. The former is caused by calibration error and device error, while the latter is caused by measurement environment.

Compared to manual inspections, the accuracy of SHM is still poor. The minimum size of detectable damage by SHM is much larger than by manual inspection methods. In addition, the measured data have the above mentioned noise and bias. Thus, the major challenge in SHM-based prognosis is how to accurately predict the damage growth when the measured data include both noise and bias. Fortunately, unlike manual inspection, SHM can provide frequent measurement of damage, allowing us to follow damage growth. This in turn, should allow us to reduce the uncertainty in the material properties that govern damage growth. As illustrated in Figure 1 the uncertainty in these properties is normally large because of variability in manufacturing and ageing of the monitored structure².

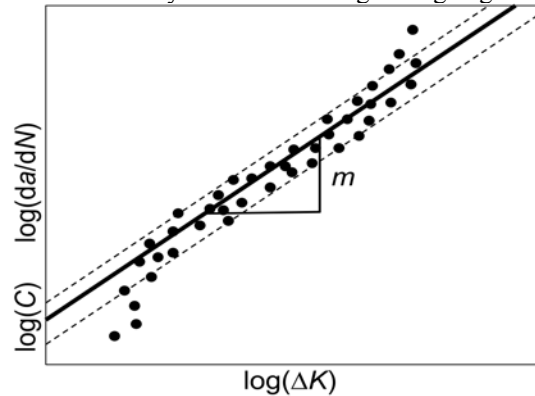


Figure 1. Illustration of Paris law parameter in a plot of crack growth rate

Another conclusion that can be drawn from that figure is that there is a very strong correlation between the parameters m and C . The goal of this paper is to compare the results obtained when using Bayesian inference to update both damage growth parameters to the results obtained when identifying only m .

The approaches are compared for a through-thickness crack in an aircraft fuselage panel which grows through cycles of pressurization and de-pressurization. A simple damage growth model, Paris law, with two damage parameters is used. However, more advanced damage growth models can also be used, which usually comes with more parameters. Using this simple model we aim to demonstrate that SHM can be used to identify the damage parameters of a particular panel. This process can be viewed as turning every aircraft into a flying fatigue laboratory. Reducing uncertainty in damage growth parameters can reduce in turn the uncertainty in predicting remaining useful life (RUL); i.e., in prognosis.

The paper is organized as follows. In Section 2, a simple damage growth model based on Paris model is presented. The current paper is based on data for the fatigue crack growth in a fuselage panel of 7075-T651 aluminum alloy. In Section 3 the results are given for the identification of the damage parameter m using Bayesian inference and the estimate on remaining useful life. In Section 4 the similar results are given for updating both m and C in a similar way. Conclusions are presented in Section 5 along with future plans.

II. Damage growth and measurement uncertainty models

A. Damage growth model

Damage in a structure starts at the microstructure level, such as dislocations and gradually grows to the level of detectable macro-cracks through nucleation and growth. Damage in the micro-structure level grows slowly, is often difficult to detect, and is not dangerous for structural safety. Thus, SHM often focuses on macro-cracks, which grow relatively quickly under fatigue loadings.

In this paper, we consider a fatigue crack growth in a fuselage panel with initial crack size a_i subjected to fatigue loads with constant amplitude due to pressurization. The hoop stress varies between a maximum value of σ to a minimum value of zero in one flight. One cycle of fatigue loading represents one flight. Like many other researchers^{3, 4}, we use the damage growth model⁵, Paris law, as

$$\frac{da}{dN} = C(\Delta K)^m \quad (1)$$

where a is the half crack size in *meter*, N the number of cycles (flights), da/dN the crack growth rate in *meter/cycle*, and ΔK the range of stress intensity factor in $MPa\sqrt{meter}$. The above model has two damage growth parameters, C and m . The plot of $\log(da/dN)$ versus $\log(\Delta K)$ becomes a straight line with m being the slope and $\log(C)$ being the y-intercept at $\Delta K = 1$.

The range ΔK of stress intensity factor for a center-cracked fuselage panel is calculated as a function of the stress $\Delta\sigma$ and the half crack length a in Eq. (2), and the hoop stress due to the pressure differential Δp is given by Eq. (3)

$$\Delta K = \Delta\sigma\sqrt{\pi a} \quad (2)$$

$$\Delta\sigma = \frac{(\Delta p)r}{t} \quad (3)$$

where r is the fuselage radius, and t is the panel thickness. Equation (2) does not include a geometric correction factor due to the finite size of the panel, and Eq. (3) does not include corrections due to the complexity of the fuselage construction, so that they are both approximate.

The number of cycles N of fatigue loading that grows a crack from the initial half crack size a_i to the current half crack size a_N can be obtained by integrating Eq. (1).

$$N = \int_{a_i}^{a_N} \frac{da}{C(\Delta\sigma\sqrt{\pi a})^m} = \frac{a_N^{1-m/2} - a_i^{1-m/2}}{C(1-m/2)(\Delta\sigma\sqrt{\pi})} \quad (4)$$

Alternatively, the half crack size a_N after N cycles of fatigue loading can be obtained by solving Eq. (4) for a_N .

$$a_N = \left(NC \left(1 - \frac{m}{2} \right) (\Delta\sigma\sqrt{\pi})^m + a_i^{1-\frac{m}{2}} \right)^{\frac{2}{2-m}} \quad (5)$$

It is assumed that the panel fails when a_N reaches a critical half crack size, a_C . Here we assume that this critical crack size is when the stress intensity factor exceeds the plane-strain fracture toughness K_{IC} . This leads to the following expression for the critical crack size (again neglecting finite panel effects)

$$a_C = \left(\frac{K_{IC}}{\Delta\sigma\sqrt{\pi}} \right)^2 \quad (6)$$

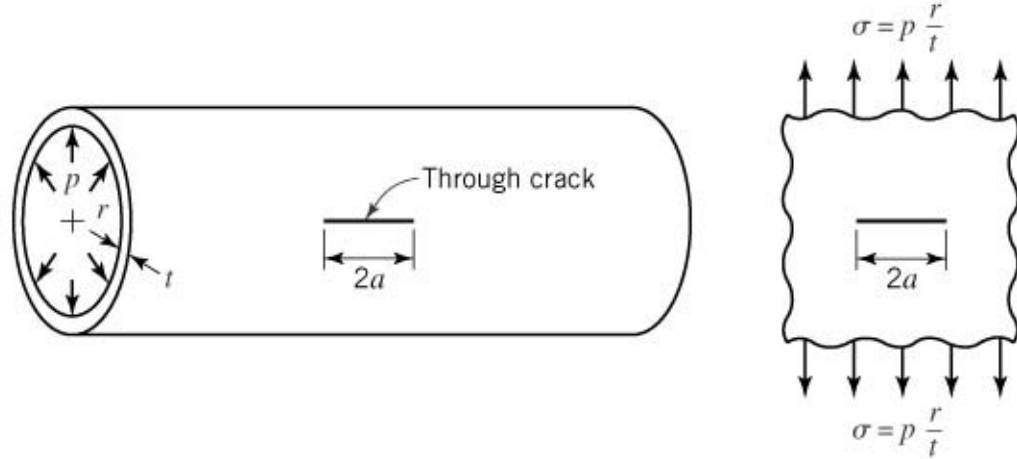


Figure 2. Through the thickness crack illustration

Typical material properties for 7075-T651 aluminum alloy are presented in Table 1. The applied fuselage pressure differential is 0.06 MPa, obtained from Niu6 and the stress is given by Eq. (3). Paris parameters m and C are obtained using a crack growth rate plot published by Newman, et al.7. Note that due to scatter in the data, the exponent m and $\log(C)$ are assumed to be uniformly distributed between the lower- and upper-bounds. In this section of the paper we ignore the correlation between the two Paris parameters8 because we try to identify one parameter assuming the other parameter is known. In the next section we will address identifying both parameters simultaneously.

Table 1. Geometry, loading and fracture parameters of 7075-T651 Aluminum alloy

Property	Pressure* Δp (MPa)	Fracture toughness K_{IC} ($MPa\sqrt{m}$)	Fuselage radius r (meters)	Paris law exponent m	Damage parameter $\log(C)$
Distribution type	Lognormal (0.06, 0.003)	Deterministic 30	Deterministic 3.25	Uniform (3.3, 4.3)	Uniform ($\log(5E-11)$, $\log(5E-10)$)

*Modeled as constant in simulations.

B. Measurement uncertainty model

In general, cracks in fuselage panels grow according to repeated pressurizations. Then, the structural health monitoring (SHM) system that is composed of sensors and actuators may detect these cracks. The fundamental function of SHM is to detect these cracks before they become unstable and dangerous.

Since no airplanes are equipped with SHM systems yet, we simulate the measured crack sizes from SHM. In general, the measured damage includes the effect of bias and noise of the sensor measurement. The former is deterministic and represents a calibration error, while the latter is random and represents a white noise. The synthetic measurement data are generated by (1) assuming that the true parameters, m_{true} and C_{true} , are known, (2) calculating the true crack growth according to Eq. (5) for a given N , and (3) adding a deterministic bias and random noise. Let a_N be the true half crack size, b the bias, and v the noise. The measured half crack size, a_N^{meas} , is then given as

$$2a_N^{meas} = 2a_N + b + v \quad (7)$$

For subsequent measurements, the bias b remains constant, while the noise v is assumed to vary uniformly with maximum range V . If the measured crack sizes are uniformly distributed due to the noise, distribution of the measured crack size can be found below:

$$a_N^{meas} \sim U\left(a_N + b/2 - V/2; a_N + b/2 + V/2\right) \quad (8)$$

The objective is to identify the true crack growth parameters using the measured crack size and its growth in Eq. (8). Once these parameters are identified, they can be used to predict the remaining useful life. Since we simulate what we called measured data because of the lack of actual data, we repeat this process multiple times to simulate the actual data statistically. Accordingly, the results will also be presented in terms of probabilistic distribution.

III. Characterization of damage property m using Bayesian updating

Depending on manufacturing and assembly processes, the actual damage parameters for individual panel can be different. For a specific panel, we assume that there exists a true value of deterministic damage parameters. In the following numerical simulation, the true damage will grow according to the true value of damage parameters. On the other hand, the measured damage size will have bias and random noise in the measurements. As a first approach to the problem we consider the distributions of m and C separately, which means that when we consider one variable as being uncertain, we assume that the other one is known. In the following section, both parameters will be identified.

From a preliminary damage growth analysis, it was found that the effect of noise in pressure p has negligible effect on damage growth because the effect of randomness is averaged out. This is true for fuselage pressurization because the variation is small. Thus, in the following analysis, the applied pressure is assumed to be deterministic, 0.06 MPa, the mean value of the distribution obtained from Niu6.

In general, the minimum size of detectable damage using SHM is much larger than that of the manual inspection. Although different SHM techniques may have different minimum detectable size, we chose an initial half crack size $a_0 = 10$ mm, which is large enough to be detected by most SHM methods. In addition, this size of damage will provide significant crack growth data between the two consecutive inspections.

The damage growth parameter m is a critical factor to determine the growth of damage. This parameter is normally measured using fatigue tests under controlled laboratory tests. However, uncertainty in this parameter is normally large not only at a material level because of variability in manufacturing and aging of the specific panel, but also on a specimen level because of variability related to testing process. It is possible to curve fit the data and estimate this parameter for the individual panel. However, curve fits do not take into account prior information on the distribution of these parameters or statistical information on the measurement uncertainty. In this paper, we use Bayesian inference to identify these parameters, which can take into account both effects.

As can be seen in Figure 1, the exponent m is the slope of the curve in the log-log scale. As a first step in developing a prognosis methodology, we assumed that the accurate value of C is known, while that of m is uncertain. Since the range of the exponent m is generally known from literature or material handbooks, we assume that the exponent is uniformly distributed between the lower- and upper-bounds. Then, the goal is to narrow the distribution of the exponent using the Bayesian statistics with measured damage sizes. The data used for the updating of material properties are crack size with uncertainty defined in Eq. (8).

Bayesian inference is based on the Bayes' theorem on conditional probability. It is used to obtain the updated (also called posterior) probability of a random variable by using new information. In this paper, since the probability distribution of m given a is of interest, we used the following form of Bayes' theorem⁹:

$$f_{updt}(m) = \frac{l(a|m)f_{ini}(m)}{\int_{-\infty}^{+\infty} l(a|m)f_{ini}(m)dm} \quad (9)$$

where, f_{ini} the assumed (or prior) probability density function (PDF) of m , f_{updt} the updated (or posterior) PDF of m and $l(a|m)$ is called the likelihood function, which is the probability of obtaining the measured damage size, a , for a given value of m .

The likelihood function is designed to integrate the information obtained from SHM measurement to the knowledge we have about the distribution of m . The details of the derivation and calculation of the likelihood function are a simplified version of the one for the joint PDF that can be found in Appendix A. Instead of assuming an analytical form of the likelihood function, we propagate uncertainty in measured crack sizes and estimated using the Monte Carlo simulation (MCS). Although this process computationally expensive, it will provide accurate information for the posterior distribution (refer to Appendix A). Figure 3 shows the updated distribution of m at various steps. It can be observed that Bayesian inference narrows down the distribution of m very accurately.

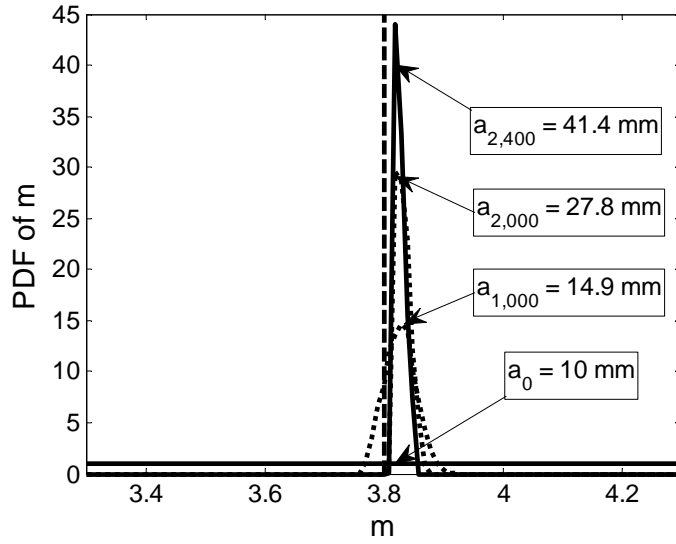


Figure 3. Probability density functions of m , illustration with one simulated set of measurements

Once the distribution of m has been identified at cycle N , it can be used to predict the remaining useful life (RUL). The distribution of RUL is calculated at every SHM measurement cycle N using MCS as well but with a larger sample than the one used to calculate the likelihood function, 50,000 true crack sizes are estimated using the following distribution in Eq. (10) and the RUL is estimated using Eq. (11) derived from Paris' law. This allows us to estimate the distribution and from there obtain the 5th percentile.

$$a_N^{true} \sim U(a_N^{meas} - b - V/2; a_N^{meas} - b + V/2) \quad (10)$$

$$N_f = \frac{a_C^{1-m/2} - (a_N^{true})^{1-m/2}}{C \left(1 - \frac{m}{2}\right) (\sigma\sqrt{\pi})} \quad (11)$$

Since we used synthetic data by adding random noise, the result may vary with different sets of data. Thus, the above process is repeated with 100 sets of measurement data and mean \pm one standard deviation intervals are plotted. In order to show the value of our method we compare RUL calculated using the actual value of m , m_{true} , and the distribution (mean \pm one standard deviation) of the 5th percentile of the distribution of RUL obtained using the updated distribution of m at each inspection, for the case of a negative bias of 2mm, and a noise of amplitude 1mm, this is shown in Figure 4. Note that the bias is ignored is assumed to be 0 for the estimation of the RUL. It can be observed that Bayesian updating allows us to improve have an estimation of RUL that converges to the true RUL from the conservative side but it is sensitive to error in the data which can be observed by the width of the distribution of RUL shown in Figure 4.

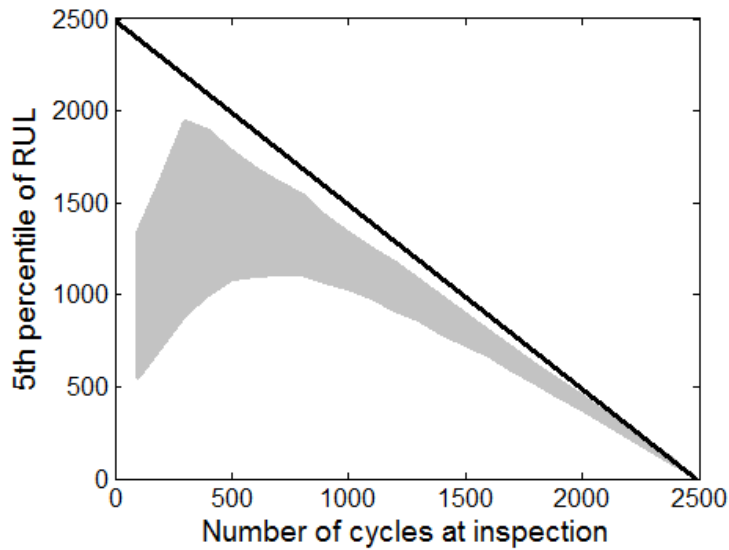


Figure 4. Distribution (mean \pm one standard deviation) of the 5th percentile of RUL for $b = -2\text{mm}$ and $V = 1\text{mm}$, using Bayesian updating to update m assuming the right value of C

One of the major advantages of SHM is that measurements can be performed frequently. Thus, the update in Eq. (9) can be performed as frequently as needed. However, since the damage grows slowly and the bias and noise of measurements are in general large, too frequent measurements may not help to narrow down the distribution of damage parameters because Bayesian inference does not give good results with large samples of data.

The previous results were obtained making the strong assumption that we know the true value of C accurately. In order to move away from that assumption let us look at the estimated RUL when C is assumed to be $1.0\text{E-}10$ in both the Bayesian inference process and the estimation of the distribution of RUL, the true value of C being $1.5\text{E-}10$. Figure 5 shows the distribution (mean \pm one standard deviation) of the 5th percentile of the estimated RUL. It can be observed that the results are very similar to the ones obtained using the true value of C . This can be explained by the fact that Bayesian identifies a value for m that compensated for the error in C the mean of the final distribution of m is 3.97 with standard deviation 0.0094.

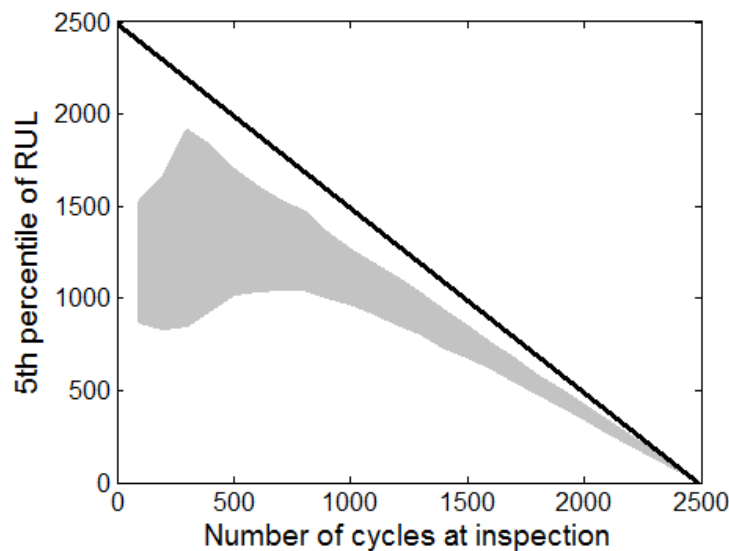


Figure 5. Distribution (mean \pm one standard deviation) of the 5th percentile of RUL for $b = -2\text{mm}$ and $V = 1\text{mm}$, using Bayesian updating to update m assuming the wrong value of C

IV. Characterization of damage properties m and C using Bayesian updating

In the previous section, Bayesian inference is used to identify a single damage growth parameter, m , and assumed the other parameter to be already known. In practice, when both parameters are unknown, Bayesian inference needs to update the joint PDF of both parameters. In general, this can be achieved by dividing the ranges of uncertain parameters into a grid and calculate the joint PDF value at each grid point. If the range is divided by 100×100 grid, the updating process includes 10,000 times calculation of likelihood, requires uncertainty propagation for given parameter values.

As can be seen in Figure 1, the exponent m is the slope of the curve in the log-log scale and C is value of da/dN at $\Delta K = 1$. Due to noise and error in experiments, the exact values of these parameters are unknown. In this section, we assume both variables as being distributed. Since the range of the variables m and C is generally known from literature or material handbooks, we assume that they are uniformly distributed between the lower- and upper-bounds generating a rectangle shaped distribution. It is assumed that these two parameters are initially uncorrelated. Therefore, the initial joint PDF is the product of individual PDFs. Then, the goal is to narrow the joint distribution using the Bayesian statistics with measured damage sizes. As to update m , the data used the joint PDF are crack sized with uncertainty defined in Eq. (8).

The Bayesian inference equation used is the same as for m , note that we chose to update $\log(C)$ in the joint distribution instead of C because of the difference in the order of magnitude:

$$f_{\text{updt}}(m, \log(C)) = \frac{l(a | m, \log(C)) f_{\text{ini}}(m, \log(C))}{\int_{-\infty}^{+\infty} l(a | m, \log(C)) f_{\text{ini}}(m, \log(C)) d m d \log(C)} \quad (12)$$

The likelihood function is designed to integrate the information obtained from SHM measurement to the knowledge we have about the distribution of the variables. The calculation of the likelihood function can be found in Appendix A. Figure 6 shows the final update of the joint distribution after 2,400 cycles, it can be observed that the correlation between m and C is very clear from that distribution even though no correlation was initially assumed. The correlation is so strong that it is possible to have an algebraic relation between the two damage growth parameters¹¹.

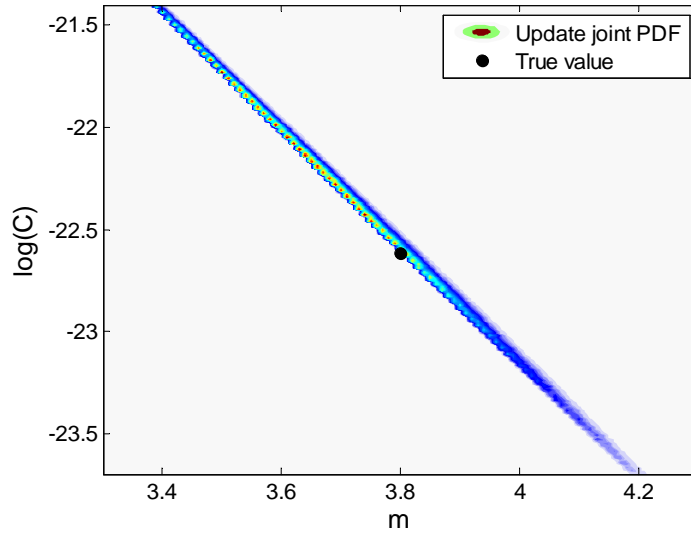


Figure 6. Final updated joint probability density function, illustration with one simulated set of measurements

It can be observed that Bayesian inference identifies the correlation between the parameters m and C , it identifies an infinite number of combination of the parameters that would lead to similar damage growth behaviors. Figure 7 shows the damage growth behavior for 5 combinations of m and C selected from the main final joint distribution, it can be observed that they lead to very similar damage growth behavior.

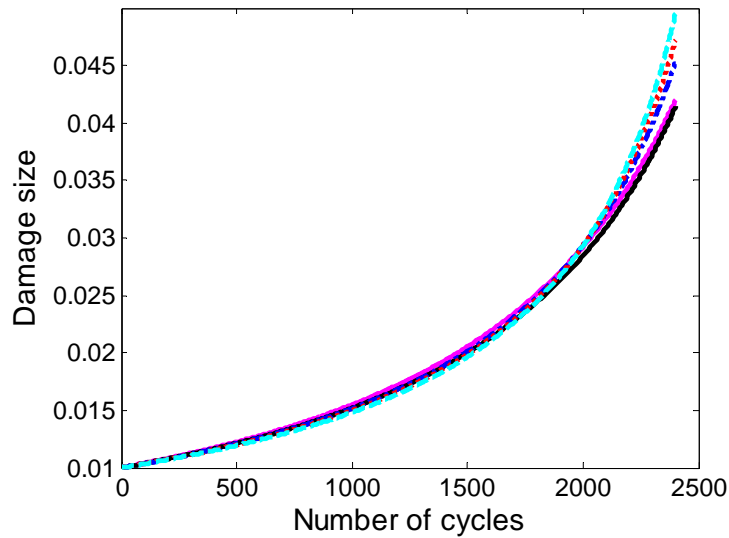


Figure 7. Damage growth for different combination of m and C

Once the joint distribution has been identified at cycle N , it can be used to predict the remaining useful life (RUL). The distribution of RUL is calculated at every SHM measurement cycle N using MCS as well but with a larger sample than the one used to calculate the likelihood function; 50,000 true crack sizes are estimated using the following distribution in Eq. (10), and the RUL is estimated using Eq. (11) with distributed parameters m and C the updated joint PDF is sampled using slice sampling. This allows us to estimate the distribution of RUL, and to obtain the 5th percentile from the distribution.

Since we used synthetic data by adding random noise, the result may vary with different sets of data. Thus, the above process is repeated with 100 sets of measurement data, and the 68% confidence interval (mean \pm one standard deviation) of 5th percentile at different N is shown in Figure 4 (gray area). In order to show the accuracy and conservativeness of the proposed method, we compare the estimated RUL with the true one, which is calculated using m_{true} , and C_{true} without considering any uncertainty (solid diagonal line). The same bias of -2mm and noise amplitude of 1mm are used. It can be observed that Bayesian updating allows us to improve the estimation of RUL compared to the RUL obtained using the handbook distribution, that estimation converges to the true RUL from the conservative side but it is sensitive to error in the data.

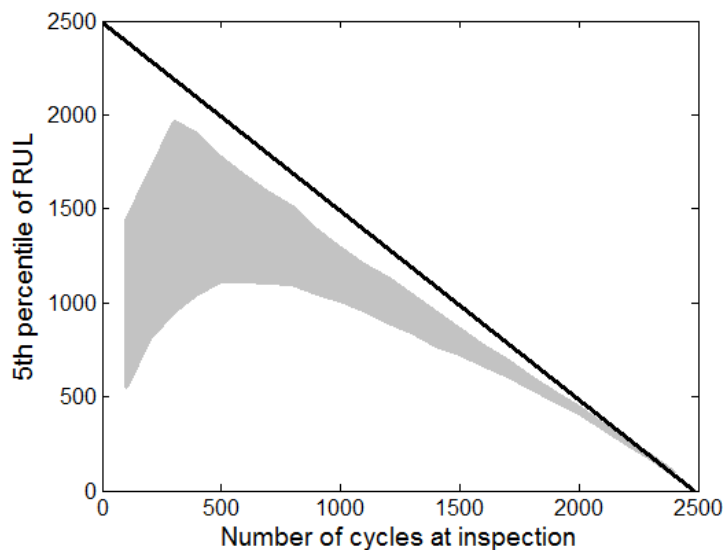


Figure 8. Distribution (mean \pm one standard deviation) of the 5th percentile of RUL for $b = -2\text{mm}$ and $V = 1\text{mm}$, using Bayesian updating

Updating the joint distribution made the correlation between m and C very clear and one of the main conclusion that can be drawn from the updated distribution is that there is not a single combination of parameters that will lead to the observed damage growth behavior. That strong correlation is also why updating one parameter while updating the other one leads to very similar results

V. Conclusions

We presented here a comparison between updating the two damage growth parameters in Paris law and updating one while assuming the other one as being constant. The main conclusion is that we do not gain accuracy in the estimation of remaining useful by updating both parameters but it is computationally more expensive. This can be explained by the strong correlation between the parameters.

That conclusion is also supported by the results obtained when updating m while making an error in the assumed value of C . In that case, the RUL is also very similar to the one obtained when updating both parameters, it is computationally much more efficient.

Note that even though the results and conclusions presented in this paper are for a specific case of bias/noise combination similar results and conclusions have been obtained for other cases.

Appendix A – Derivation of the likelihood for Bayesian inference

The idea is to identify the damage parameters m or C from the measured half crack size that is contaminated by measurement errors. In order to do that, we compare the measurements to the simulated crack size defined above. In order to use the information in Bayes law, we need to estimate the likelihood $l(a|m, C)$ that for a given set of material properties m and C , or in other words:

$$d = a_N^{sim} - a_N^{meas} = 0 \quad (13)$$

If we have analytical expressions for the PDFs of a_N^{meas} and a_N^{sim} , and we use them to obtain the PDF of d , then the value of this PDF at $d = 0$ is the likelihood function. Since this rarely happens, we will use MCS, and we will use as likelihood function

$$l(a | m, C) = P(|d| \leq \epsilon) \quad (14)$$

Note that the integration over ϵ is just a normalizing constant that is taken care of by the normalization in the Bayesian formulation.

If we calculate $l(a|m, C)$ purely by sampling a_N^{meas} and a_N^{sim} , then the tolerance ϵ needs to be large enough to include enough sample points to reduce the sampling error to acceptable levels. On the other hand if ϵ is large, we will incur errors due to nonlinearity in the likelihood function.

We will assume now that the measurement error that controls a_N^{meas} is independent of the modeling errors that control a_N^{sim} . In that case, separable sampling can be performed by comparing all possible combinations of two individual samples.

The PDF of a_N^{sim} is not available analytically, because it is obtained from propagation of uncertainties through an analysis code. On the other hand, the measurement errors are assumed rather than propagated, and they are here assumed to be uniform in a bounded region. We will now investigate how we can take advantage of the given distribution of a_N^{meas} in order to improve the efficiency or accuracy of the sampling. In this case a_N^{meas} and a_N^{sim} are scalar, such that

$$l(a | m, C) = P(|d| \leq \epsilon) = 1 - P(d + \epsilon \leq 0) - P(d - \epsilon \geq 0) \quad (15)$$

Using conditional expectation on the second term on the right-hand side we obtain

$$\begin{aligned} P(d - \epsilon \geq 0) &= P(a_N^{sim} - a_N^{meas} - \epsilon \geq 0) \\ &= \int_{a_N^{sim}} P(a_N^{sim} - a_N^{meas} - \epsilon \geq 0) f_{sim}(a_N^{sim}) da_N^{sim} \\ &= \int_{a_N^{sim}} F_{meas}(a_N^{sim} - \epsilon) f_{sim}(a_N^{sim}) da_N^{sim} \end{aligned} \quad (16)$$

where $f_{sim}(x)$ is the PDF of a_N^{sim} and $F_{sim}(x)$ is the CDF of a_N^{sim} . The last relation is obtained from the definition of CDF; i.e., by considering a_N^{meas} as the only random variable, $P(a_N^{meas} \leq a_N^{sim} - \epsilon) = F_{meas}(a_N^{sim} - \epsilon)$. Similarly, the first term can be written as

$$\begin{aligned}
P(d + \epsilon \geq 0) &= \int_{a_N^{sim}} P(a_N^{sim} - a_N^{meas} + \epsilon \geq 0) f_{sim}(a_N^{sim}) da_N^{sim} \\
&= \int_{a_N^{sim}} F_{meas}(a_N^{sim} + \epsilon) f_{sim}(a_N^{sim}) da_N^{sim}
\end{aligned} \tag{17}$$

Thus, by combining Eqs. (16) and (17), the likelihood can be written as

$$\begin{aligned}
l(a | m, C) &= \int_{a_N^{sim}} [F_{meas}(a_N^{sim} + \epsilon) - F_{meas}(a_N^{sim} - \epsilon)] f_{sim}(a_N^{sim}) da_N^{sim} \\
&\approx 2\epsilon \int_{a_N^{sim}} f_{meas}(a_N^{sim}) f_{sim}(a_N^{sim}) da_N^{sim}
\end{aligned} \tag{18}$$

where the central finite difference approximation is used in the second relation, which becomes exact when $\epsilon \rightarrow 0$. As explained before, since the posterior PDF will be normalized, the coefficient 2ϵ can be ignored. The above expression is in particular convenient for separable MCS because the analytical expression of $f_{meas}(x)$ is known, and $f_{sim}(x)$ can be evaluated by propagating uncertainty through numerical simulation. Let M be the number of samples in MCS, the likelihood can then be calculated by

$$\begin{aligned}
l(a | m, C) &= \int_{\Delta a_N^{sim}} f_{meas}(a_N^{sim}) f_{sim}(a_N^{sim}) da_N^{sim} \\
&\approx \frac{1}{M} \sum_{i=1}^M f_{meas}(a_{N,i}^{sim})
\end{aligned} \tag{19}$$

In the literature¹⁰, Gaussian function is often assumed for the likelihood function. In addition, the expression of this function remains unchanged throughout the entire process. However, Figure 9 shows that the likelihood function is quite different from the Gaussian function and it varies at different crack sizes. Since the uncertainty structure of the posterior distribution strongly depends on the likelihood function in Bayesian inference, the error in the likelihood calculation directly affects the accuracy of the posterior distribution.

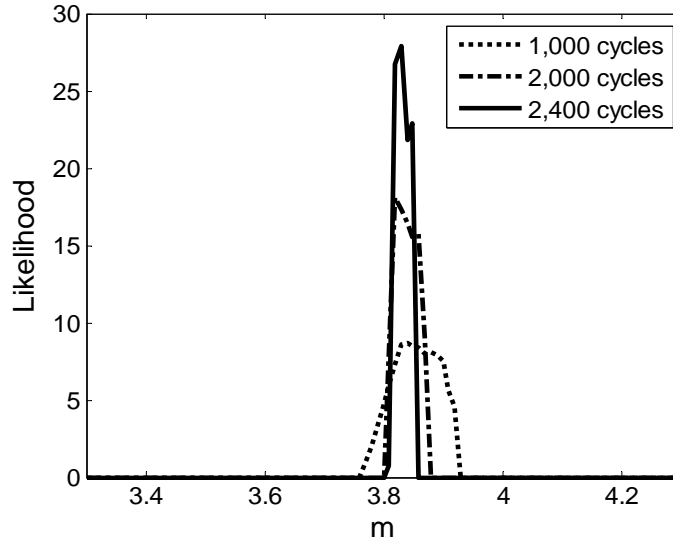
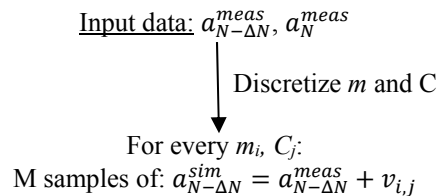


Figure 9. Likelihood function for one set of measurements at various number of cycles

In the case presented here $f_{meas}(a_{N-\Delta N,i}^{sim})$ is the PDF corresponding to the triangular distribution defined in Eq. (9). We give below the detailed algorithm of the Bayesian procedure at the N^{th} inspection



With $v_{i,j} \sim U(-V, V)$

$$a_N^{sim} = \left[\Delta N C_j \left(1 - \frac{m_i}{2} \right) (\Delta \sigma \sqrt{\pi})^{m_i} + (a_{N-\Delta N}^{sim})^{1-\frac{m_i}{2}} \right]^{\frac{2}{2-m_i}}$$
$$l(\Delta a | m_i, C_j) = \frac{1}{M} \sum_{i=1}^M f_{meas}(a_{N,i,j}^{sim})$$

Acknowledgment

This work was supported by the Air Force Office of Scientific Research under Grant FA9550-07-1-0018 and by the NASA under Grant NNX08AC334.

References

- ¹Wang, L. and Yuan, F. G., “Damage identification in a composite plate using prestack reverse-time migration technique”, *Structural Health Monitoring*, vol. 4, pp. 195-211, 2005.
- ²DuQuesnay, D.L. and Underhill, P.R., “Fatigue life scatter in 7xxx series aluminum alloys”, *International Journal of Fatigue*, Elsevier, 2009.
- ³Harkness, H. H., “Computational methods for fracture mechanics and probabilistic fatigue”. Ph.D. thesis, the Northwestern University, Evanston, IL, 199
- ⁴Lin, K. Y., Rusk, D. T. and Du, J. J., “Equivalent level of safety approach to damage-tolerant aircraft structural design”, *Journal of Aircraft*, vol. 39, pp. 167-174, 2002.
- ⁵Paris, P. C., Tada, H. and Donald, J. K., “Service load fatigue damage—a historical perspective”, *International Journal of Fatigue*, vol. 21, pp. 35-46, 1999.
- ⁶Niu, M., "Airframe Structural Design," in *Fatigue, Damage Tolerance and Fail-Safe Design*, Connilit Press LTD., Ed. Hong Kong, pp. 538-570, 1990.
- ⁷Newman, J. C., Phillips, E. P. and Swain, M. H., “Fatigue-life prediction methodology using small-crack theory”, *International Journal of Fatigue*, vol. 21, pp. 109-119, 1999.
- ⁸Carpinteri, A., Paggi, M., “Are the Paris' law parameters dependent on each other?” - *Frattura ed Integrità Strutturale*, 2008
- ⁹An, J., Acar, E., Haftka, R. T., Kim, N. H., Ifju, P. G. and Johnson, T.F., “Being Conservative with a Limited Number of Test Results”, *Journal of Aircraft*, vol. 45, pp. 1969-1975, 2008.
- ¹⁰Li, G., Yuan, F. G., Haftka, R. T. and Kim, N. H., “Bayesian segmentation for damage image using MRF prior”, *Sensors and Smart Structures Technologies for Civil, Mechanical, and Aerospace Systems, SPIE Conference*, San Diego, CA, USA vol. 7292 pp. 72920J-12, 2009
- ¹¹Sinclair, G. B. and Pierie, R. V., “On obtaining fatigue crack growth parameters from the literature,” *International Journal of Fatigue*, Vol. 12, No. 1, pp. 57-62, 1990